

**Applied Meteorology Unit
(AMU)**

**Quarterly Report
Third Quarter FY-01**

Contract NAS10-96018

31 July 2001

**ENSCO, Inc.
1980 N. Atlantic Ave., Suite 230
Cocoa Beach, FL 32931
(321) 853-8202 (AMU)
(321) 783-9735**

This page is intentionally left blank

Distribution:

NASA HQ/Q/F. Gregory
NASA KSC/AA/R. Bridges
NASA KSC/MK/J. Halsell
NASA KSC/PH/D. King
NASA KSC/PH/E. Mango
NASA KSC/PH/M. Leinbach
NASA KSC/PH/M. Wetmore
NASA KSC/PH-A/J. Guidi
NASA KSC/YA/J. Heald
NASA KSC/YA-C/D. Bartine
NASA KSC/YA-D/H. Delgado
NASA KSC/YA-D/J. Madura
NASA KSC/YA-D/F. Merceret
NASA KSC/YA-C/G. Allen
NASA JSC/DA8/W. Hale
NASA JSC/MA/R. Dittmore
NASA JSC/MS2/C. Boykin
NASA JSC/ZS8/F. Brody
NASA MSFC/ED03/S. Pearson
NASA MSFC/ED44/D. Johnson
NASA MSFC/ED44/B. Roberts
NASA MSFC/ED44/G. Jasper
NASA MSFC/MP01/A. McCool
NASA MSFC/MP71/S. Glover
45 WS/CC/N. Wyse
45 WS/DO/M. Christie
45 WS/DOR/D. Beberwyk
45 WS/DOR/D. McCabe
45 WS/DOR/J. Sardonia
45 WS/DOR/J. Tumbiolo
45 WS/DOR/E. Priselac
45 WS/DOR/J. Weems
45 WS/SY/D. Harms
45 WS/SYR/W. Roeder
45 WS/SYA/B. Boyd
45 OG/CC/D. Mitchell
45 LG/CC/S. Fancher
45 LG/LGP/R. Fore
CSR 7000/M. Maier
CSR 4140/H. Herring
45 SW/SESL/D. Berlinrut
SMC/CWP/M. Coolidge
SMC/CWP/T. Knox
SMC/CWP/R. Bailey
SMC/CWP (PRC)/P. Conant
Hq AFSPC/DORW/S. Carr
Hq AFWA/CC/C. French
Hq AFWA/DNX/E. Bensman
Hq AFWA/DN/N. Feldman
Hq USAF/XOW/H. Tileston
Hq AFRL/XPPR/B. Bauman
Office of the Federal Coordinator for Meteorological Services and Supporting Research

SMC/AXEW/L. Hagerman
NOAA “W/NP”/L. Uccellini
NOAA/OAR/SSMC-I/J. Golden
NOAA/NWS/OST12/SSMC2/J. McQueen
NOAA Office of Military Affairs/L. Freeman
Aerospace Corp/T. Adang
NWS Melbourne/B. Hagemeyer
NWS Southern Region HQ/“W/SRH”/X. W. Proenza
NWS Southern Region HQ/“W/SR3”/D. Smith
NSSL/D. Forsyth
NWS/“W/OSD5”/B. Saffle
FSU Department of Meteorology/P. Ray
NCAR/J. Wilson
NCAR/Y. H. Kuo
30 WS/SY/C. Crosiar
30 WS/CC/P. Boerlage
30 SW/XP/J. Hetrick
NOAA/ERL/FSL/J. McGinley
ENSCO Contracts/E. Lambert

Executive Summary

This report summarizes the Applied Meteorology Unit (AMU) activities for the third quarter of Fiscal Year 2001 (April – June 2001). A detailed project schedule is included in the Appendix.

Ms. Lambert completed work on the Statistical Short-Range Forecast Tools task to develop and test short-range ceiling forecast equations for use in support of Shuttle landings at the Shuttle Landing Facility. She conducted hypothesis tests to determine the statistical significance of the improvement of the observations-based (OBS) equations over the persistence climatology (PCL) equations, and tested the forecast skill of the equations using different probability cutoff values for a Yes/No forecast. The hypothesis tests showed that the improvement was significant beyond the 99% confidence level. The probability value tests showed that the optimal forecast probability cutoff value to use in operations is likely between 0.4 and 0.5. The final report is in external review.

Dr. Short and Mr. Wheeler began work on the Improved Anvil Forecasting Phase II task to develop an anvil forecasting tool that will aid forecasters in predicting the triggered lightning Launch Commit Criteria (LCC) violation probability. Mr. Wheeler created software to archive routinely available satellite, forecast model and upper air data on a daily basis. Dr. Short analyzed the data from days on which thunderstorm anvils occurred. The preliminary findings confirm the results of a previous study done by Mr. Sardonia of the 45th Weather Squadron (45 WS), that the wind speed/direction and relative humidity in the 300 - 150 mb layer are strong indicators of the resultant length and lifetime of thunderstorm anvils. The preliminary results, however, are based on warm season daytime anvils only.

Dr. Manobianco and Mr. Wheeler completed transitioning the new Stratified Logistic Thunderstorm Index (SLTI) developed at the Air Force Institute of Technology. The SLTI will replace the Neumann-Pfeffer Thunderstorm Probability Index (NPTPI) currently used by the 45 WS. Initial results with SLTI show improvement over NPTPI, and the 45 WS requested that the new SLTI be implemented before the 2001 warm season. Dr. Manobianco and Mr. Wheeler finished coding the SLTI, and it was transitioned to the 45 WS in early June. Dr. Manobianco discovered and corrected an error in reading the 6-day thunderstorm persistence data. Mr. Wheeler recompiled and tested the SLTI software and then forwarded the updated executable to the 45 WS.

The AMU was tasked to upgrade the software used to superimpose the location of the Airborne Field Mill (ABFM) research aircraft on WSR-74C radar images in a Graphical User Interface (GUI). The ABFM program is designed to improve the lightning LCC for Shuttle and expendable launch vehicles. Mr. Wheeler provided technical support during the experiment in June 2001 by trouble-shooting problems with the GUI and participating in twice-daily weather briefings.

Mr. Case distributed the final report describing the methodology and results of the Meso-Model Evaluation task. The output from the Regional Atmospheric Modeling System (RAMS) component of the Eastern Range Dispersion Assessment System (ERDAS) was evaluated for its accuracy in forecasting several meteorological phenomena, including the East Coast Sea Breeze (ECSB). The methodology and results of the RAMS ECSB forecast verification for the 1999 and 2000 warm seasons are summarized in this report. Mr. Case found that RAMS demonstrates good utility in predicting the occurrence and timing of the ECSB.

Mr. Case also began work on Phase IV of the Local Data Integration System (LDIS) task. The goal of the LDIS task is to generate high-resolution weather analysis products that may enhance the operational forecasters' understanding of the current state of the atmosphere, resulting in improved short-term forecasts. Phase IV involves including additional real-time observational datasets, fine tuning the analysis configuration to improve continuity and blending of observations, and improving real-time graphics capabilities.

Mr. Dianic continued work on the extension and enhancement of the ERDAS RAMS Evaluation task to improve the archived database and to perform sensitivity tests to identify the possible cause(s) of the model cold bias. He fixed a problem in the software that caused the verification GUI to crash periodically, and improved various aspects of the GUI interface. He also incorporated a program that calculates error statistics for RAMS forecasts in order to generate intermediate files for use by the verification GUI.

Table of Contents

Executive Summary	iii
SPECIAL NOTICE TO READERS	1
1. BACKGROUND	1
2. AMU ACCOMPLISHMENTS DURING THE PAST QUARTER.....	1
2.1 TASK 003 SHORT-TERM FORECAST IMPROVEMENT	1
SUBTASK 3 Statistical Short-Range Forecast Tools (Ms. Lambert)	1
SUBTASK 5 Improved Anvil Forecasting Phase II (Dr. Short and Mr. Wheeler)	6
SUBTASK 6 Neumann-Pfeffer Index Replacement (Dr. Manobianco and Mr. Wheeler).....	9
2.2 TASK 004 INSTRUMENTATION AND MEASUREMENT.....	10
SUBTASK 12.1 Aircraft Position Radar Overlay (Mr. Wheeler and Mr. Dianic).....	10
SUBTASK 13 MiniSODAR™ Evaluation (Dr. Short and Mr. Wheeler).....	11
SUBTASK 5 I&M and RSA Support (Dr. Manobianco, Mr. Case, and Mr. Wheeler)	11
2.3 TASK 005 MESOSCALE MODELING.....	12
SUBTASK 8 Meso-Model Evaluation (Mr. Case).....	12
SUBTASK 10 Local Data Integration System Phase IV (Mr. Case).....	16
SUBTASK 11 Extension / Enhancement of the ERDAS RAMS Evaluation (Mr. Case and Mr. Dianic)	17
2.4 AMU CHIEF'S TECHNICAL ACTIVITIES (DR. MERCERET).....	17
2.5 TASK 001 AMU OPERATIONS	17
List of Acronyms.....	20
Appendix A.....	22

SPECIAL NOTICE TO READERS

Applied Meteorology Unit (AMU) Quarterly Reports are now available on the Wide World Web (WWW) at <http://science.ksc.nasa.gov/amu/home.html>.

The AMU Quarterly Reports are also available in electronic format via email. If anyone on the current distribution would like to be added to the email list, please send your email address to Winifred Lambert (321-853-8130, lambert.winifred@ensco.com). If any of your mailing information changes or if you would like to be removed from the distribution list, please notify Frank Merceret (321-867-0818, francis.merceret-1@ksc.nasa.gov) or Winifred Lambert (321-853-8130, lambert.winifred@ensco.com).

1. BACKGROUND

The AMU has been in operation since September 1991. Tasking is determined annually with reviews at least semi-annually. The progress being made in each task is discussed in Section 2 with the primary AMU point of contact reflected on each task and/or subtask. A list of acronyms used in this report immediately follows Section 2.

2. AMU ACCOMPLISHMENTS DURING THE PAST QUARTER

2.1 TASK 003 SHORT-TERM FORECAST IMPROVEMENT

SUBTASK 3 STATISTICAL SHORT-RANGE FORECAST TOOLS (MS. LAMBERT)

The forecast cloud ceiling at the Shuttle Landing Facility (SLF) is a critical element in determining whether a GO or NO GO should be issued for a Space Shuttle landing. However, the Spaceflight Meteorology Group (SMG) forecasters have found that ceiling is a difficult parameter to forecast. The goal of this task is to develop short-range ceiling forecast equations to be used in support of Shuttle landings. Ms. Lambert is using a 19-year record (1979–1997) of hourly surface observations from the SLF and several stations in east-central Florida to develop these equations. The equation development is centered on the ceiling thresholds defined by the Shuttle Flight Rules (FR) (NASA/JSC 1997a) and shown in Table 1.

<i>Ceiling Threshold</i>	<i>Flight Rule</i>
< 5000 ft	Return to Launch Site (RTLS)
< 8000 ft	End of Mission (EOM)
< 10 000 ft	Navigation Aid Degradation

Ms. Lambert conducted hypothesis testing to determine the statistical significance of the improvement of the observations-based (OBS) equations over the persistence climatology (PCL) equations, and calculated probability of detection (POD) and false alarm rate (FAR) scores using different probability cutoff values for a Yes/No forecast.

Hypothesis Testing

While it was important to show that the OBS equations produced improved forecasts over that of the PCL equations, it was also important to know whether that improvement was statistically significant. Statistical significance was determined through the use of hypothesis testing. A null hypothesis was defined first, then the testing determined whether that hypothesis could be rejected. For this study, the null hypothesis was that the mean of the differences between the OBS and PCL mean square error (MSE) values was 0, which would indicate that the OBS equation improvement was not significant and that use of the PCL equations would produce forecasts as accurate as the OBS equations.

Hypothesis tests are broadly classified into parametric and nonparametric tests. A parametric test is used when the data are represented by a known theoretical distribution. A nonparametric test does not require the data to be in any particular distribution. In order to choose an appropriate test, the MSE differences were calculated by subtracting PCL MSEs from their corresponding OBS MSEs and the distributions of the differences were examined by lead time and ceiling category. Figure 1 shows the distribution of the 24 MSE differences for 2-hour forecasts of ceilings < 8000 feet. Most distributions, like that shown in Figure 1, did not bear similarity to any theoretical distribution. It is important to note here that most of the differences were negative, indicating that the OBS MSEs were smaller than the PCL MSEs. This re-confirms the previous finding that the OBS equations produce more accurate forecasts than the PCL equations.

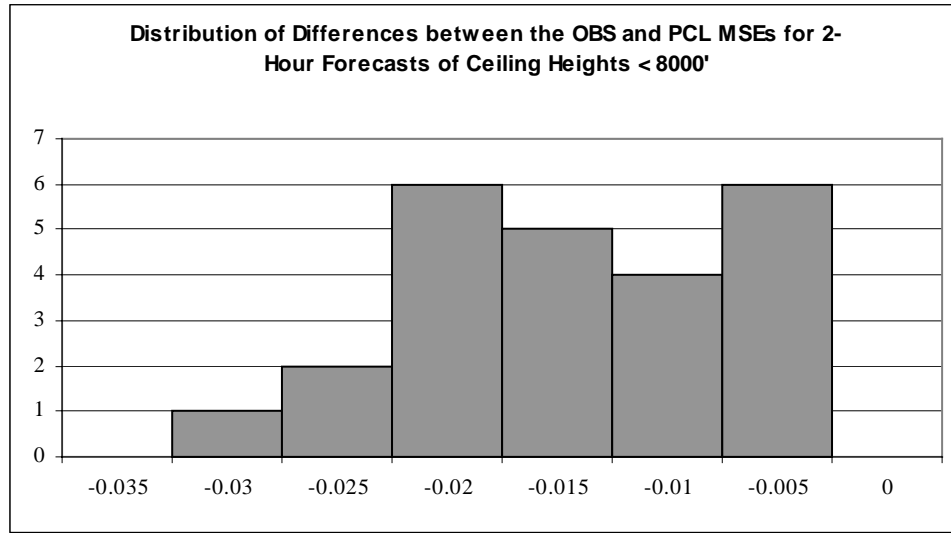


Figure 1. Distribution of differences between the OBS and PCL MSE values for the 24 hourly equations for 2-hour forecasts of ceilings < 8000 feet. The value under each bin is the upper bound of that bin's range.

Given the non-similarity to any theoretical distributions, a nonparametric test called the Wilcoxon Signed Rank test (Wilks 1995; Insightful Corp. 1999) was chosen to determine statistical significance. This test calculated the difference between corresponding pairs of OBS and PCL MSE values and used these differences to determine if the mean of the differences was not equal to 0 (Wilks 1995). The critical output value from the test was the p-value. The p-value represents the probability of error involved in accepting that the difference between the two MSEs is valid. The smaller the p-value, the less likely the difference is due to chance and the more probable that the difference is significant. The common convention is to use a p-value of 0.05 as the threshold value to accept or reject the null hypothesis, indicating a 95% confidence that the mean of the differences is not equal to 0.

A total of nine tests were conducted using the MSE values generated from forecasts with the independent dataset. The corresponding OBS and PCL MSE values from the 24 valid times in each lead time/ceiling category group were input to the algorithm. All p-values were only slightly larger than 0, on the order of 1e-7 to 1e-8. The smallness of the p-value suggested that the null hypothesis, which was that the mean of the differences between the OBS and PCL MSEs was 0, could be rejected with greater than 99% confidence. The alternative hypothesis, that the OBS MSEs were significantly less than the PCL MSEs, was accepted with the same confidence. Therefore, the improvement in forecast accuracy by the OBS equations over the PCL equations was statistically significant.

Probability Cutoff for Yes/No Forecasts

In previous calculations of POD and FAR, 0.5 was used as the probability cutoff between Yes/No forecasts in the standard contingency table (Figure 2). The use of this value produced POD and FAR scores that indicated good forecast accuracy. The appropriate value for operations, however, would depend on whether the user wished to maximize POD or minimize FAR. To assist in this decision, calculations were done for 11 cutoff values from 0 to 1 in 0.1 increments, inclusive. The resulting POD and FAR scores for the independent data are shown in Figure 3. The values plotted were averaged over valid time and ceiling height category, resulting in a mean value for each lead time. All POD and FAR values decreased with increasing probability cutoff value. The 1-hour forecasts produced the highest POD and lowest FAR values. The POD values decreased slowly from 1 at the 0.0 probability cutoff to 0.83 at the 0.4 cutoff, remained constant through 0.5 and dropped rapidly after the 0.6 cutoff. The FAR values also decreased, but did so more rapidly from the 0.0 probability cutoff through 0.4. They remained somewhat constant through 0.6 and decreased slowly thereafter. The values for the other two lead time categories decreased similarly, although in a more linear fashion.

		<i>Observed</i>	
		Yes	No
<i>Forecast</i>	Yes	x	z
	No	y	w

$$POD = \frac{x}{x + y}$$

$$FAR = \frac{z}{x + z}$$

Figure 2. The standard contingency table used in calculating several measures of accuracy of the binary forecasts. Each letter represents the number of times an event was x) forecast and observed, z) forecast but not observed, y) not forecast but observed, and w) not forecast and not observed. The equations for POD and FAR are shown to the right of the table.

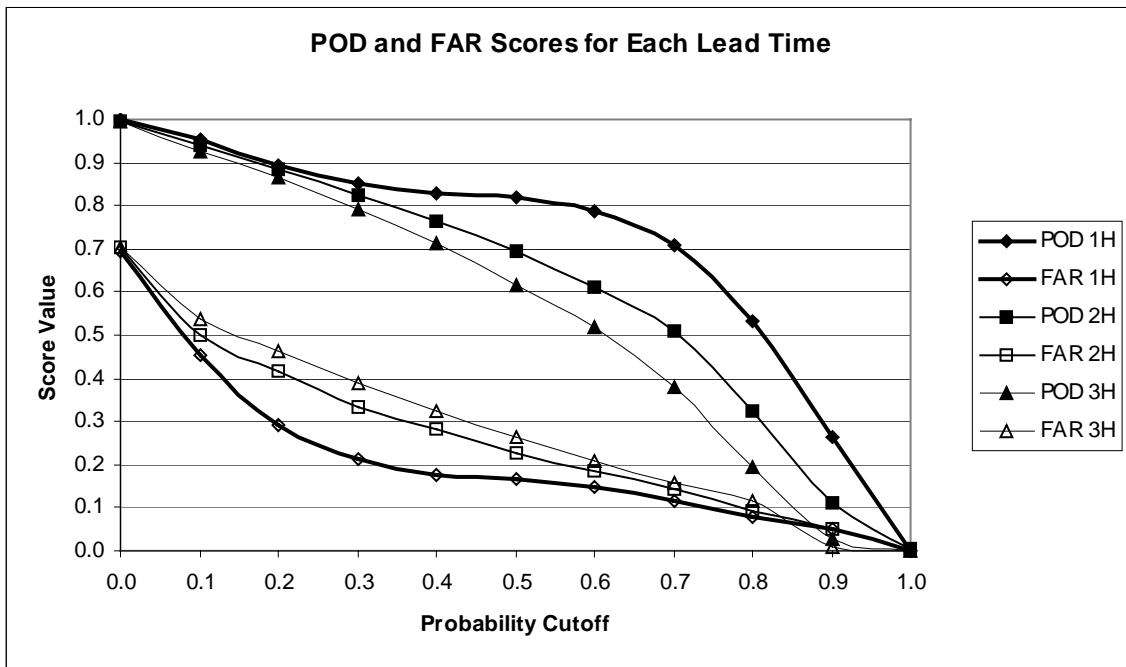


Figure 3. The average POD and FAR values for the three lead times at each probability cutoff using the independent dataset. The bold lines represent the 1-hour forecast values, the medium-weight lines represent the 2-hour forecast values, and the light-weight lines represent the 3-hour forecast values.

Other measures of accuracy and skill were also needed to determine an appropriate cutoff value or range of values. Four other measures were calculated using the contingency table in Figure 2. Wilks (1995) recommended using the threat score (TS) and bias (B) ratio as good indicators of the appropriate cutoff value. When choosing a probability cutoff value, Wilks (1995) suggests choosing the probability where TS is maximized and/or where B=1. These two scores are calculated as (see Figure 2 for definitions of x, y, and z):

$$TS = \frac{x}{x + z + y}, \text{ and } B = \frac{x + z}{x + y}.$$

The other two measures employed to help determine the best probability cutoff were the Hit Rate (HR) and Kuipers Skill Score (KSS) (Wilks 1995). They were calculated to help narrow down or confirm the probability cutoff values chosen by the TS and B scores. Where the TS is the percent of correct Yes forecasts, the HR is the percent of all correct forecasts, Yes and No. The best HR is 1 and the worst is 0. The KSS indicates whether the forecast is better than, equal to, or worse than random forecasting. A perfect forecast is indicated by KSS = 1, a forecast similar to a random forecast is indicated by KSS = 0, and KSS < 0 indicates a forecast that is worse than a random forecast. These two scores are calculated as (see Figure 2 for definitions of x, y, z, and w):

$$HR = \frac{x + w}{w + x + y + z}, \text{ and } KSS = \frac{xw - zy}{(x + y)(z + w)}.$$

Figure 4 shows the average values of the four measures for all equations with a 1-hour lead time. The TS was maximized between the probability values of 0.4 and 0.5, and B =1 at the same location. The value of TS at the maximum was 0.7, indicating 70% correct Yes forecasts when using a probability cutoff between 0.4 and 0.5. The co-location of B = 1 and the TS maximum indicated that using a probability value between 0.4 and 0.5 as the cutoff would produce the most accurate forecasts. This was confirmed by the HR and KSS scores. The HR maximum was 0.9 at the 0.5 probability value indicating that 90% of the forecasts were correct, and the KSS maximum was 0.76 at the 0.4 probability value. A positive KSS value close to 1 indicated that these forecasts were much more accurate than random forecasts.

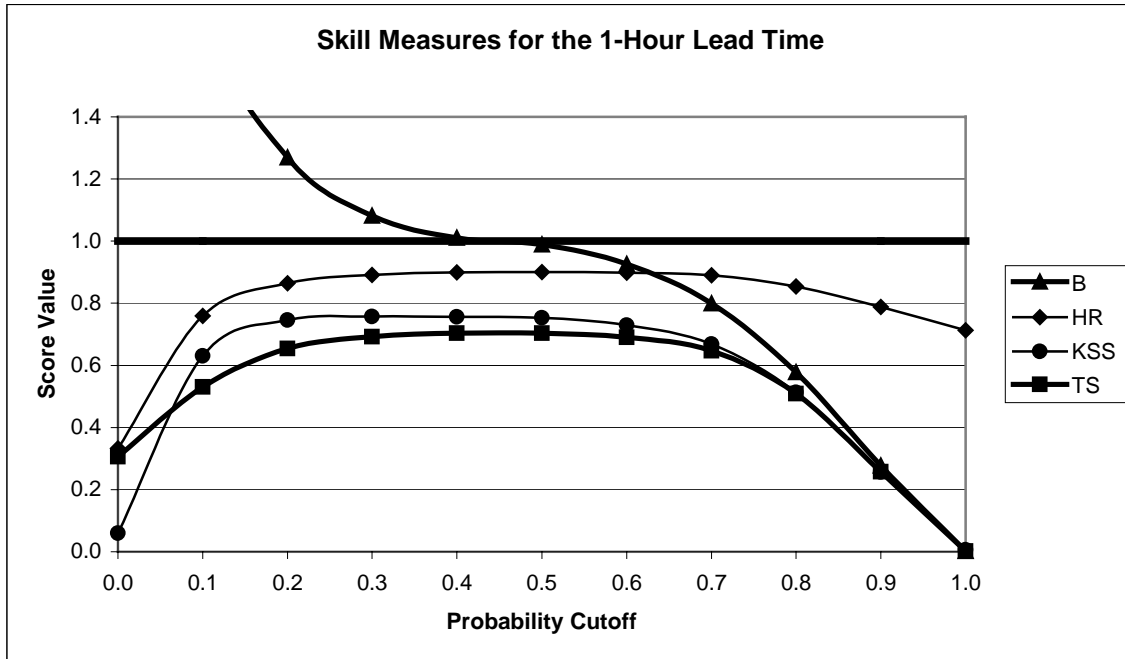


Figure 4. The B, HR, KSS, and TS values for the 1-hour lead time. The gridline for Score Value = 1 is bold to emphasize where B = 1, and the B and TS curves are bold since they are used to determine the appropriate cutoff value according to Wilks (1995). The scale of the vertical axis was truncated to emphasize the smaller values of the other skill and accuracy measures. The maximum B value was 3.4 at probability cutoff 0.0.

Graphs for the other two lead times are not shown for brevity, but an analysis of the results for all three lead times indicated that the appropriate probability cutoff values decreased with lead time, but tended to be between 0.4 and 0.5. Since these values were calculated from forecasts using the independent data, they are good indicator of the appropriate probability cutoff values to be used in operations. Ultimately, operational use of the equations will determine the most appropriate cutoff values, but these tests provide a starting point.

Final Report

Ms. Lambert completed a second draft of the final report that had gone through AMU internal review and is currently undergoing external review. The final report will be distributed in August 2001. For more information or a copy of the final report, contact Ms. Lambert at lambert.winifred@ensco.com or 321-853-8130.

References

Insightful Corporation, 1999: *S-PLUS® 2000 User's Guide*, Insightful Corp., Seattle, WA. 558 pp.

NASA/JSC, 1997a: NASA Operational Shuttle Flight Rules (NSTS 12820), Final June 6, 1996, PCN-11 December 7, 2000, Vol A, Section 2.1.1-6. NASA/Johnson Space Center, 2-11 – 2-33. [Available from JSC/DA8, Houston, TX 77058.]

Wilks, D. S., 1995: *Statistical Methods in the Atmospheric Sciences*. Academic Press, Inc., San Diego, CA, 467 pp.

SUBTASK 5 IMPROVED ANVIL FORECASTING PHASE II (DR. SHORT AND MR. WHEELER)

An objective technique for forecasting the horizontal extent of anvil clouds generated by thunderstorm activity is needed to assist forecasters in predicting the probability of violating the triggered lightning Launch Commit Criteria (LCC). An anvil cloud can extend 100 miles or more from its parent thunderstorm complex depending on the winds aloft, and can serve as a long distance conduit for lightning discharges. Charging mechanisms in anvil clouds are complex; but, in general, the observed structure is a positively charged center surrounded by negatively charged exterior screening layers above and below. The screening layers can have an adverse effect on the ability of the Launch Pad Lightning Warning System (LPLWS) to detect electrification in an anvil above the network. Anvil clouds can become detached from their parent thunderstorm but still carry hazardous electrical charges (Garner et al. 1997).

The 45th Weather Squadron (45 WS) Launch Weather Officers (LWOs) have identified anvil forecasting as one of the most challenging tasks when attempting to predict the triggered lightning LCC violation probability. The SMG forecasters have reiterated this difficulty when evaluating Space Shuttle FR. Phase I of this task (Lambert 2000) established the technical feasibility of developing an observations-based forecasting technique, given the promising relationships found by the 45 WS between anvil length and lifetime and the average wind speed/direction and moisture content in the anvil layer. The goals of Phase II are to 1) build upon the results of Phase I with data collection and analysis that will increase the sample size of anvil cases to improve the reliability of resulting statistics and 2) develop objective tools for forecasting the occurrence of anvil clouds over the Kennedy Space Center (KSC) and Cape Canaveral Air Force Station (CCAFS) area with lead times of 36 hours or less.

Dr. Short and Mr. Wheeler initiated Phase II of this task in late April 2001 by developing a list of routinely available satellite, forecast model and upper air data to be archived on a daily basis beginning in May 2001. The initial data list, based on results of the Phase I study and discussions with forecasters from the 45 WS, SMG and National Weather Service in Melbourne, FL (NWS MLB) will be revised, if necessary, in accordance with further recommendations from the forecasters. Mr. Wheeler created daily file transfer scripts to download Geostationary Operational Environmental Satellite (GOES) sounding data, field and point data from the Eta forecast model, and Rapid Update Cycle (RUC) analysis and forecast data. He also completed routines for daily archiving of satellite, surface observations and lightning data through the Meteorological Interactive Data Display System (MIDDS). These routines will allow the AMU to generate a complete set of data from which to extract specific cases for the task.

Method of Analysis

The AMU is following the analysis procedure developed by Mr. Sardonia of the 45 WS in a pilot study of anvil clouds conducted during 1999 and 2000 and documented by Lambert (2000). The procedure is to use visible satellite imagery to record the horizontal extent of mature anvils and to determine upper level winds and humidity in the anvil layer from nearby rawinsonde data. Mr. Sardonia determined that the average wind speed and humidity in the layer from 300 to 150 mb were strongly correlated with anvil lengths. The AMU added five additional parameters: 1) the direction from the point where the parent thunderstorm complex formed to the end of the mature anvil, 2) the coordinates of the point where the parent thunderstorm complex originated, 3) the wind direction in the upper tropospheric layer, 4) the wind speed in a lower tropospheric layer from 900 to 500 mb, and 5) the wind direction in the lower tropospheric layer. The lower tropospheric layer was added to include information affecting the motion of thunderstorms during their formative stages.

Anvil cloud properties are measured in a subjective analysis of visible satellite imagery from channel 1 on GOES, number 8 (GOES-8), 0.55-0.75 μm , with a spatial resolution of 1 km. GOES-8 digital data is archived every 15 to 30 minutes and analyzed within a few days using the Man-Computer-Interactive-Data-Analysis-System (McIDAS). The McIDAS software provides the user with customized image enhancement capabilities that facilitate interpretation of satellite imagery in terms of cloud features. Anvil clouds originating from small clusters of thunderstorms during the warm season are readily evident in time loops of the visible imagery. These extensive anvil clouds, classified as *cirrostratus cumulonimbogenitus*, rapidly expand tens of kilometers or more in a manner consistent with the wind flow in the upper troposphere, in the layer from about 300 to 150 mb. The anvil cloud is highly reflective during its growing and mature phases, obscuring views of the surface and lower clouds. Infrared

imagery (channel 4, 10.2-11.2 μm) indicates effective black body temperatures colder than 240K in anvil clouds, consistent with atmospheric temperatures in the upper troposphere.

Within one to three hours after it first appears, the nontransparent portion of the anvil cloud reaches its greatest extent, defined here as the mature stage. After reaching its mature stage the anvil cloud begins to dissipate, revealing surface features and lower clouds beneath it in the visible imagery. At the time of maturity, a record is made of the maximum distance from the nontransparent edge of the anvil cloud to the location where the parent cluster of thunderstorms originated, along with the coordinates of the originating location. Atmospheric wind speeds and directions are determined for each anvil by using data from the nearest rawinsonde station that preceded the anvil observation by less than 12 hours. Wind speed and wind direction are averaged for an upper tropospheric layer most likely to contain the anvil, 300 to 150 mb, and a mid-tropospheric layer most likely to influence the motion of thunderstorm cells, 900 to 500 mb. The dew point depression is also recorded for the upper tropospheric layer from the same rawinsonde observation. An anvil case day is defined as one in which the life history of at least three anvil clouds were clearly evident and measured from satellite imagery, consistent with Mr. Sardonía's study. At times, anvil-type clouds less than 30 km long are seen in two or three consecutive frames of the GOES-8 visible imagery. Features of this type are not included in the analysis presented below.

The following sections provide a detailed analysis of anvil case days during May and June 2001. The interpretation of transport lifetimes is based on the pilot study that was performed by Mr. Sardonía and documented in the Phase I final report (Lambert 2000).

May/June 2001 Analysis Results

During the months of May and June 2001, Dr. Short determined the life cycle of 93 anvil clouds in GOES-8 visible imagery on 30 anvil case days. He computed daily averages of anvil distance, anvil orientation, wind speed and wind direction in the lower and upper troposphere, and dew point depression in the upper troposphere. Figure 5a shows a scatter diagram of daily averages of layer-averaged wind speed in the upper troposphere versus anvil distance. A linear regression of the two variables indicates an intercept of about 25 nm and a slope of 1.9 nm/kt. The regression relationship explains 76% of the variance of anvil distance by the wind speed. The non-zero intercept indicates that anvil clouds can be expected to reach a scale of about 25 nm when the upper level wind speed is near zero, just due to the inertia and divergence of the cloud mass itself. Refinement of the regression relationship by incorporation of additional variables will be explored using statistical analysis tools in S-PLUS[®].

Figure 5b shows a scatter diagram of wind speed versus anvil length-offset, where the offset is 25 nm. The solid sloping lines indicate time scales that are consistent with the wind speeds and anvil lengths. For example, a length of 100 nm and a wind speed of 50 kts indicate a time-scale of two hours. The time scale is referred to as an effective transport lifetime, indicating the approximate time it took the anvil to reach its maximum extent at maturity. The average effective transport lifetime is 1.87 hours with a standard deviation of 0.51 hours.

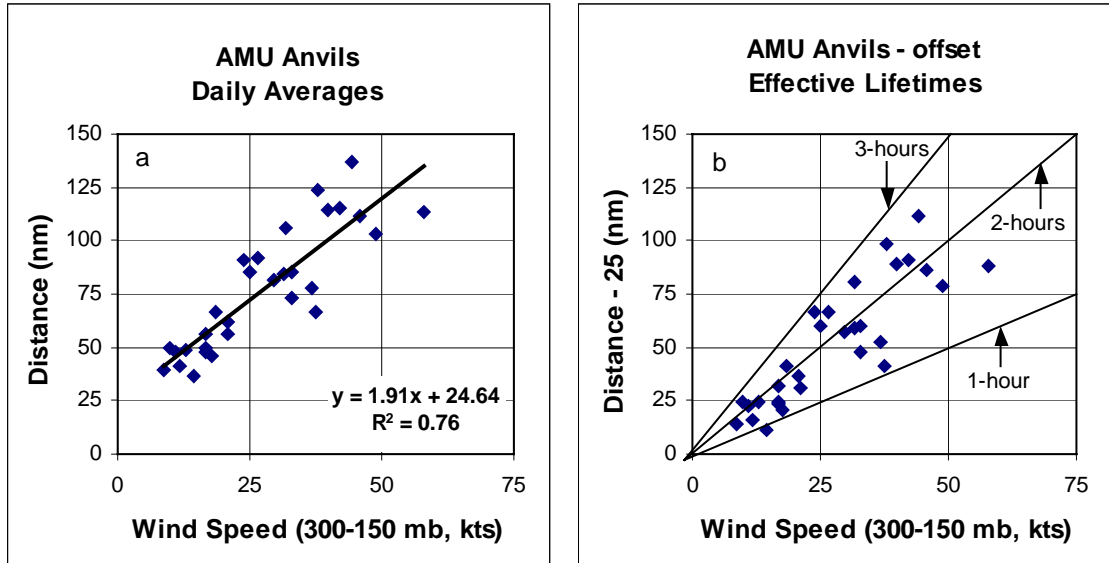


Figure 5. Daily averages of upper tropospheric wind speed versus anvil characteristics. a) Daily averages of wind speed and anvil distance: b) Daily averages of wind speed versus anvil distance - offset, where the offset, 25 nm, was determined from the linear regression in a). The sloping lines denote effective transport lifetimes, calculated from the ratio of distance-offset to wind speed.

Figure 6a shows a scatter diagram of layer-averaged upper tropospheric wind direction and anvil orientation for the 30 case days described above. The layer-averaged upper winds were from the southwest through northwest for most of the case days with a few days showing winds with an easterly component. The average anvil direction for the dataset is 277° , only 3° greater than the average upper tropospheric wind direction. This indicates that the upper level wind direction gives a nearly unbiased indication of anvil orientation. Figure 6b shows a scatter diagram of layer-averaged upper tropospheric wind speed versus the difference between anvil orientation and upper wind direction. The directional difference, or error, is largest at wind speeds below 15 kts and has a standard deviation of 15° for wind speeds above 15 kts. The decrease in directional errors with increasing wind speed is consistent with greater accuracy in measuring the bearing between two points as the distance between them increases, provided the location errors of the points are independent of their separation distance.

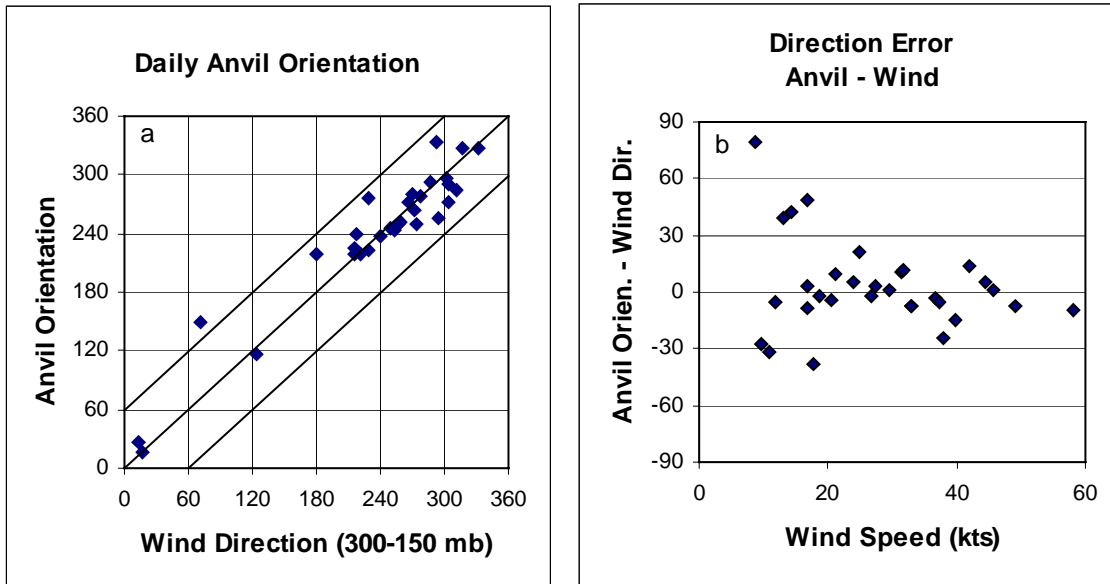


Figure 6. Daily averages of relationships between anvil orientation, wind speed and wind direction. a) Daily anvil orientation versus wind direction: b) Deviation of anvil orientation from wind direction versus wind speed. Note that the deviations are largest at the lowest wind speeds.

The preliminary findings from the Phase II AMU study confirm the results of Mr. Sardonia's pilot study, documented by the AMU in Phase I (Lambert 2000). One important caveat regarding the present study is that it is based on warm season anvils thus far, whereas Mr. Sardonia's study included winter cases. A further caveat applying to both studies is that they are based on analysis of visible imagery during the daylight hours. Nighttime anvils have not been studied.

The AMU will request a telephone conference with 45 WS, SMG, and NWS MLB forecasters in early August to discuss the findings documented above and to obtain feedback regarding the future direction of the task.

References

Garner, T., R. Lafosse, D. G. Bellue, and E. Priselac, 1997: Problems associated with identifying, observing, and forecasting detached thunderstorm anvils for Space Shuttle operations. *7th Conference on Aviation, Range and Aerospace Meteorology*, Long Beach, CA, Amer. Meteor. Soc., 302 - 306.

Lambert, W. C., 2000: Improved anvil forecasting: Phase I Final Report. NASA Contractor Report CR-2000-208573, Kennedy Space Center, FL, 24 pp. [Available from ENSCO, Inc., 1980 N. Atlantic Ave., Suite 230, Cocoa Beach, FL, 32931].

SUBTASK 6 NEUMANN-PFEFFER INDEX REPLACEMENT (DR. MANOBIANCO AND MR. WHEELER)

The Air Force Institute of Technology (AFIT) has developed a Stratified Logistic Thunderstorm Index (SLTI) to replace the Neumann-Pfeffer Thunderstorm Probability Index (NPTPI). Initial results show improvement over NPTPI, and the 45 WS requested that the new SLTI be implemented for forecaster use before the 2001 warm season.

Dr. Manobianco and Mr. Wheeler finished coding the SLTI by late May. It was transitioned to the 45 WS in early June. Dr. Manobianco discovered and corrected a minor error in reading the 6-day thunderstorm persistence data. Mr. Wheeler recompiled and tested the SLTI software and then forwarded the updated executable to the 45 WS. A memorandum describing the previously performed work, the required input parameters, and format of the SLTI output (Figure 7) was distributed.

```

Stratified Logistic Thunderstorm Index (SLTI)
replaces Neumann-Pfeffer Thunderstorm Index (THUNDER)

SLTI developed by Air Force Institute of Technology

SLTI converted for operational use by
Applied Meteorology Unit (AMU)

K Index = 36.80
Thompson Index = 42.00
800-600 mb Avg. RH = 0.71
6-Day thunderstorm persistence = 110111
Wind Speed (m/s) & Direction @ 900 mb = 4.1 288.
Wind Speed (m/s) & Direction @ 850 mb = 2.6 285.
Wind Speed (m/s) & Direction @ 700 mb = 3.6 348.
Wind Speed (m/s) & Direction @ 600 mb = 5.7 2.

Year= 2001 Month= 7 Day= 10 T-storm Prob= 0.50

Specify input data file

```

Figure 7. Example of the Stratified Logistic Thunderstorm Index (SLTI) output.

2.2 TASK 004 INSTRUMENTATION AND MEASUREMENT

SUBTASK 12.1 AIRCRAFT POSITION RADAR OVERLAY (MR. WHEELER AND MR. DIANIC)

The aircraft position radar overlay task is funded by KSC under AMU option hours. The AMU was tasked to superimpose the location of the research aircraft from the Airborne Field Mill (ABFM) experiment on Weather Surveillance Radar, model 74C (WSR-74C) SIGMET radar images. The ABFM experiment collected data to allow safe revision of the lightning LCC to provide greater launch availability. The AMU was tasked to install and test needed software updates to the Graphical User Interface (GUI) (Figure 8) and data acquisition prior to the June 2001 ABFM deployment.

The summer ABFM deployment began in late May 2001 with significant convection and anvil formation occurring on its first day. Anvil formation and data collection opportunities continued almost through the end of the deployment. The average flight lasted approximately three hours. Excluding ferry flight and calibration runs, more than 60 hours of data were collected.

Mr. Wheeler provided real-time support for the ABFM project throughout the experiment and Mr. Dianic modified the software to make it more robust. Mr. Wheeler participated in twice-daily weather briefings and collected radar, satellite and flight track, and other data during each flight. These data will be used in the analysis phase of the project, which will take 12-18 months.

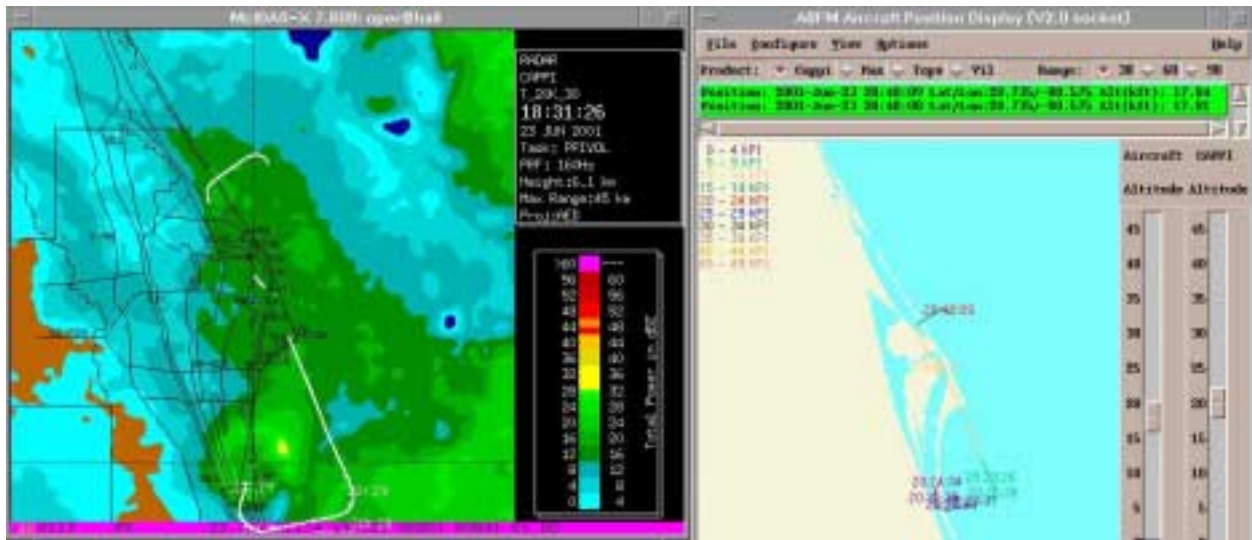


Figure 8. Example of the Airborne Field Mill Graphical User Interface (ABFM GUI) display. The WSR-74C data with the aircraft track (white line) is in the left panel. The user display interface showing the aircraft track, position and time stamp data from aircraft, aircraft altitude (right side, left slide bar) and altitude of displayed radar display (right side, right slide bar).

SUBTASK 13 MINISODAR™ EVALUATION (DR. SHORT AND MR. WHEELER)

Dr. Short and Mr. Wheeler continued the data collection and analysis of MiniSODAR™ and wind tower data. A seven-month archive of MiniSODAR™ and tower data for the months of October, November, and December 2000, and January, February, March, April 2001 now exists. A meeting of 45 WS, Range Standardization and Automation (RSA), Computer Sciences Raytheon (CSR) and AMU personnel was conducted on 25 April to discuss task methodology, data quality control and instrument maintenance. As a result of this meeting, Dr. Merceret suspended AMU work on this task pending resolution of questions regarding permission to use and publish data, and instrument maintenance.

SUBTASK 5 I&M AND RSA SUPPORT (DR. MANOBIANCO AND MR. WHEELER)

In April, Dr. Manobianco and Mr. Wheeler met with Ms. Katherine Winters (45 WS), Mr. Timothy Wilfong (Lockheed Martin), and Mr. Charles Fain (45th Logistics Group; 45 LG) to discuss AMU connectivity to RSA weather systems. The meeting participants reviewed AMU hardware/software and weather data requirements necessary to perform AMU tasks. These requirements will be used to update the latest RSA proposed solution for AMU connectivity and weather display systems. Mr. Wheeler attended a 45 WS meeting to gather information about latest RSA incremental delivery plan for the RSA weather product. The discussion centered on what capabilities and functionalities would be needed in the new RSA weather product to allow the phase out of the current MIDDS weather display system.

In June, Drs. Manobianco and Merceret and Mr. Wheeler met with Mr. Wilfong and representatives from the 45 WS, 45 LG, and CSR to discuss the AMU hardware configuration and equipment location. The AMU will have a fully functional NOAAPort receiver, model server, and Advanced Weather Interactive Processing System (AWIPS) file server. All local and national data will be transmitted to the AMU via file transfer protocol. Mr. Wheeler will send Mr. Wilfong a list of AMU equipment that must be moved and/or removed, the disposition of the AMU Weather Surveillance Radar 1988 Doppler (WSR-88D) Principle User Processor and recommendations for a mass storage backup system.

Table 2. AMU hours used in support of the I&M and RSA task in the third quarter of FY 2001 and total hours since July 1996.	
<i>Quarterly Task Support (hours)</i>	<i>Total Task Support (hours)</i>
8.5	320.0

2.3 TASK 005 MESOSCALE MODELING

SUBTASK 8 MESO-MODEL EVALUATION (MR. CASE)

The Eastern Range Dispersion Assessment System (ERDAS) is designed to provide emergency response guidance to the 45th Space Wing/Range Safety (45 SW/SE) in support of operations at the Eastern Range in the event of an accidental hazardous material release or an aborted vehicle launch. ERDAS uses the Regional Atmospheric Modeling System (RAMS) numerical weather prediction (NWP) model to generate prognostic wind and temperature fields for input into ERDAS diffusion algorithms. The RAMS model is run twice per day and generates 24-hour forecasts initialized at 0000 and 1200 UTC. In addition to winds and temperatures, RAMS predicts a number of other meteorological quantities on four nested grids with horizontal grid spacing of 60, 15, 5, and 1.25 km, respectively. Since the 1.25-km grid is centered over KSC/CCAFS, real-time RAMS forecasts provide an opportunity for improved weather forecasting in support of space operations through high-resolution NWP over the complex land-water interfaces of KSC/CCAFS. The 45 SW/SE and the 45 WS have tasked the AMU to evaluate the accuracy of RAMS for all seasons and under various weather regimes during 1999 and 2000.

Mr. Case submitted two papers to the American Meteorological Society (AMS) joint conference on Numerical Weather Prediction and Weather Analysis and Forecasting that will be presented in Ft. Lauderdale, FL from 30 July to 2 August. In addition, the ERDAS RAMS final report was completed, published, and distributed. The final report contains a summary and description of the objective and subjective evaluations conducted for the 1999 warm season (May to August), the 1999-2000 cool season (November to March), and the 2000 warm season (May to September). The objective evaluation consists of point error statistics for both the 1999-2000 cool and 2000 warm seasons at several observation locations, and point error statistics at the KSC/CCAFS wind towers under various meteorological regimes for the 2000 warm-season. The subjective evaluation consists of a verification of the onset and propagation of the East Coast Sea Breeze (ECSB) for the 1999 and 2000 warm-seasons, and a precipitation and thunderstorm initiation verification for the 2000 warm season. The following sub-sections present the ECSB evaluation methodology and summarize the final RAMS ECSB verification statistics for the 1999 and 2000 Florida warm seasons.

Methodology for the Verification of Sea breezes

The AMU conducted the sea-breeze verification at several individual KSC/CCAFS wind towers. All archived RAMS forecasts from May–August 1999 and from May–September 2000 were examined to verify the forecast ECSB. Point forecasts and observations were examined at 12 selected KSC/CCAFS wind towers, representing three different zones in the wind-tower network (the coastal barrier islands, Merritt Island, and mainland Florida, as shown in Figure 9). In each zone, four towers were identified in a north-south orientation that contained the most data for both the 1999 and 2000 Florida warm seasons. Twelve-panel graphical plots (meteograms) displaying both the forecast and observed wind direction and speed were generated for all RAMS forecast cycles to verify the occurrence and timing of the ECSB at each selected wind tower.

The AMU utilized both GOES-8 visible imagery and WSR-74C reflectivity data to identify the occurrence of the ECSB on a given day. A sea breeze is typically accompanied by a sharp clearing line and reflectivity fine line that propagate westward with the sea breeze. To determine the occurrence and timing of the sea-breeze passage, the AMU examined each KSC/CCAFS wind tower for a development of or wind-shift to an onshore wind component (wind direction between 335° and 155°, the approximate orientation of the Florida coastline). The definition of an onshore versus offshore wind at coastal towers 1 and 3 varied from the rest of the towers due to the specific

orientation of the coastline along the tip of Cape Canaveral (Figure 9). At these towers, onshore flow was defined as a wind direction between 335° (NW) and 180° (S) at tower 1 and between 335° (NW) and 200° (SSW) at tower 3. As a result, both of these towers have a larger range of wind directions that are onshore compared to the other towers.

During easterly flow regimes, a sea-breeze passage was determined by a distinct increase in the negative (easterly) u-wind at each wind tower. These same wind criteria were then applied to the ERDAS RAMS forecasts interpolated to each wind tower location to determine the forecast ECSB passage. Finally, the occurrence of a forecast and observed sea breeze was verified on a per-tower basis in order to incorporate a spatial verification of the ECSB on a given day. This methodology not only demands a high level of accuracy in the model predictions, but it also increases the size of the database.

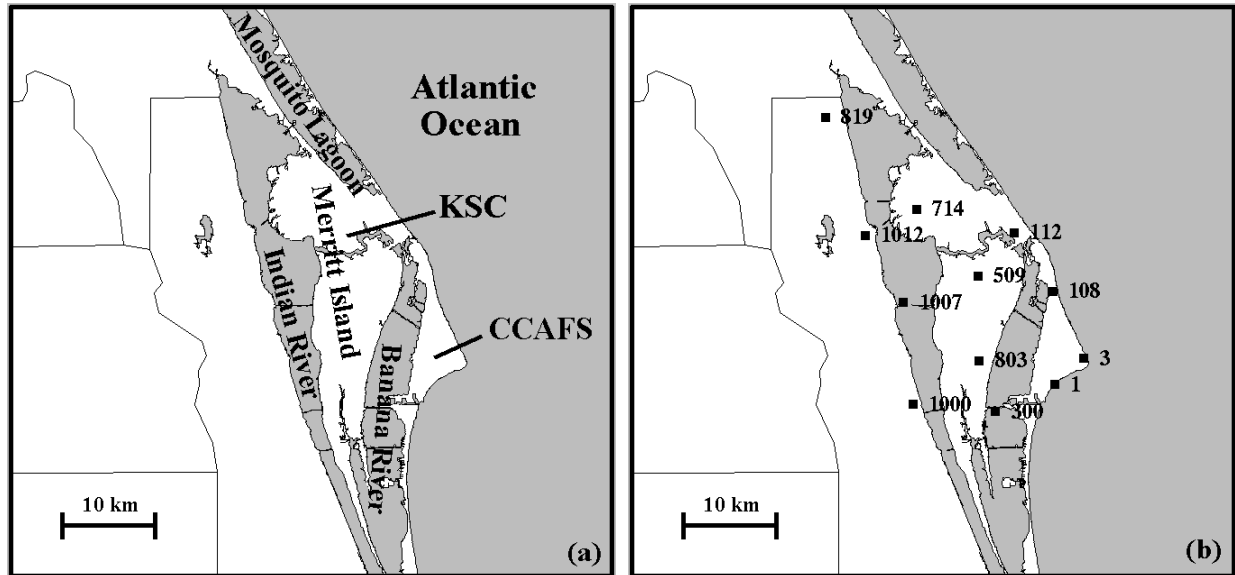


Figure 9. A plot of the geographic locations of KSC, CCAFS, the local water bodies surrounding KSC/CCAFS, and the 12 KSC/CCAFS wind towers used for the east coast sea-breeze subjective verification. The labels of geographical locations are given in (a) and the wind tower locations are shown in (b).

A 2×2 contingency table was used to summarize the ECSB verification statistics based on the occurrence of both an observed and forecast ECSB at any of the 12 KSC/CCAFS towers. A “hit” is defined as the occurrence of both an observed and forecast sea-breeze passage at a particular KSC/CCAFS tower. Because RAMS forecast output is available once per hour, the AMU verified the timing of the onset and movement of the sea breeze to the nearest hour at each of the 12 KSC/CCAFS towers. Table 3 represents a sample 2×2 contingency table from which a variety of categorical and skill scores can be computed to measure forecast performance. The total number of correct forecasts is given by x in the upper left corner (forecast and observed = yes) and w in the lower right corner (forecast and observed = no). The number of forecast misses is given in the lower left portion of the table (forecast = no, observed = yes) and the number of false alarm forecasts is given in the upper right corner (forecast = yes, observed = no).

Table 3. A sample 2×2 contingency table for the evaluation of a forecast element is shown from which categorical and skill scores are computed (see text).		
	<i>Observed = Yes</i>	<i>Observed = No</i>
<i>Forecast = Yes</i>	x	z
<i>Forecast = No</i>	y	w
Number of correct forecasts = (x+w)		
Number of false alarm forecasts = z		
Number of forecast misses = y		

From the contingency table, a variety of categorical and skill scores can be calculated as defined in Schaefer (1990) and Doswell *et al.* (1990). These scores include the bias, POD, FAR, Critical Success Index (CSI), and the Heidke Skill Score (HSS). Using the variables in Table 3, these scores are defined as follows:

$$\text{Bias} = \frac{x + z}{x + y},$$

$$\text{POD} = \frac{x}{x + y},$$

$$\text{FAR} = \frac{z}{x + z},$$

$$\text{CSI} = \frac{x}{x + y + z},$$

$$\text{HSS} = \frac{2(xw - yz)}{y^2 + z^2 + 2xw + (y + z)(x + w)}.$$

Given the occurrence of a weather element, the POD is the percentage of time that RAMS correctly forecasted that element. The FAR is the percentage of time that RAMS incorrectly forecasted a weather element when none occurred. The CSI measures the ratio of the number of hits to the number of events plus the number of false alarms. The HSS provides a benchmark of the model performance compared to random forecasting (HSS=0). Higher POD, CSI, and HSS combined with a low FAR are associated with better performance of the model forecasts. In a perfect forecast, the bias, POD, CSI, and HSS are equal to 1 and the FAR is 0. The next sub-section provides a summary of the error statistics and categorical and skill scores for the subjective verification of the forecast ECSB. The error statistics generated for the sea-breeze timing verification include root mean square (RMS) error and bias (in hours) in addition to the categorical and skill scores.

Verification of RAMS Forecast Sea breezes for the 1999 and 2000 Florida Warm Seasons

Tables 4 and 5 show a contingency table and categorical and skill scores for the occurrence of an ECSB passage at the 12 selected KSC/CCAFS towers during the 1999 and 2000 warm seasons. These tables represent nine months of data (May–August 1999 and May–September 2000) for both the 0000 and 1200 UTC RAMS forecast cycles. If no data were missing, the theoretical maximum number of elements in Table 4 is 3312 for each forecast cycle (276 days multiplied by 12 wind towers); however, several forecasts were missing and several towers experienced various outages, particularly during the 2000 warm season. In addition, when either the 0000 or 1200 UTC forecast was missing on a given day, the other forecast cycle was removed to maintain the exact same database for comparison between the two forecast cycles. As a result, about 75% (2469 elements) of the possible data are available for the overall sea-breeze evaluation.

Based on the results in Tables 4 and 5, observed sea breezes occurred at the 12 wind towers about 65% of the time (1609 out of 2469 elements), of which RAMS correctly predicted 86% of them in the 0000 UTC cycle and 98% of them in the 1200 UTC cycle, according to the POD in Table 5. The probability of a null event (PON, not shown), the score analogous to POD for correct “no” forecasts of a sea breeze, indicates that both forecast cycles correctly predict non-sea breeze days only 66–70% of the time. The FAR is 16% for both the 0000 and 1200 UTC RAMS cycles. As a result of the higher POD in the 1200 UTC forecasts, this RAMS cycle has the highest CSI and HSS. The HSS of 0.69 indicates that RAMS demonstrates a significant amount of utility in predicting the occurrence of the ECSB. By applying statistical significance tests following the methodology used in Hamill (1999), each of the differences in scores between the 0000 and 1200 UTC forecasts were determined to be statistically significant at the 99% confidence level, except for the FAR.

In the instances when a correct yes forecast of a sea breeze occurred, the timing errors were determined at each of the wind towers during the 9-month evaluation period. Table 6 summarizes the timing error statistics for all the correct yes forecasts of a sea breeze for both the 0000 and 1200 UTC cycles. In general, the RMS error ranges from 1.5–2.1 h for each category of wind towers. The errors are smallest at the coastal towers and largest at the mainland towers, but the variation between these locations is less than 0.5 h, which is smaller than the data-sampling rate of once per hour. In all instances the bias is -0.2 or -0.3 h, which is negligible compared to the sampling rate.

Table 4. Contingency tables of the occurrence of the operational RAMS forecast versus observed sea breeze, verified at each of the 12 selected KSC/CCAFS towers of Figure 9 during the 1999 and 2000 Florida warm seasons.		
0000 UTC Forecast Cycle	Observed Sea Breeze	No Observed Sea Breeze
Forecast Sea Breeze	1381	261
No Forecast Sea Breeze	228	599
1200 UTC Forecast Cycle	Observed Sea Breeze	No Observed Sea Breeze
Forecast Sea Breeze	1575	293
No Forecast Sea Breeze	34	567

Table 5. Categorical and skill scores of RAMS forecast versus observed sea breeze during the 1999 and 2000 Florida warm seasons, associated with the contingencies in Table 4.		
Parameter	0000 UTC Forecast Cycle	1200 UTC Forecast Cycle
Probability of Detection	0.86	0.98
False Alarm Rate	0.16	0.16
Bias	1.02	1.16
Critical Success Index	0.74	0.83
Heidke Skill Score	0.56	0.69

Table 6. A summary of timing error statistics for the May–August 1999 and May–September 2000 evaluation periods are given for the subjective sea breeze verification performed for the 12 KSC/CCAFS tower locations of Figure 9. The RMS error and bias are shown in units of hours for the 0000 UTC and 1200 UTC forecast runs.

Location	Statistic	0000 UTC Cycle	1200 UTC Cycle
Coastal Towers	RMS Error	1.8	1.5
	Bias	-0.3	-0.3
Merritt Island Towers	RMS Error	1.9	1.7
	Bias	-0.3	-0.2
Mainland Towers	RMS Error	2.1	1.9
	Bias	-0.3	-0.2

For more information or to obtain a copy of the interim or final report, contact Mr. Jonathan Case at 321-853-8264 or by email at case.jonathan@ensco.com.

References

Doswell, C. A., R. Davies-Jones, and D. Keller, 1990: On summary measures of skill in rare event forecasting based on contingency tables. *Wea. Forecasting*, **5**, 576-585.

Hamill, T. M., 1999: Hypothesis tests for evaluating numerical precipitation forecasts. *Wea. Forecasting*, **14**, 155-167.

Schaefer, J. T., 1990: The critical success index as an indicator of warning skill. *Wea. Forecasting*, **5**, 570-575.

SUBTASK 10 LOCAL DATA INTEGRATION SYSTEM PHASE IV (MR. CASE)

The Local Data Integration System (LDIS) task emerged out of the need to simplify short-term weather forecasting in support of launch, landing, and ground operations. The complexity of creating short-term forecasts has increased due to the variety and disparate characteristics of available weather observations. Therefore, the goal of the LDIS task is to generate high-resolution weather analysis products that may enhance the operational forecasters’ understanding of the current state of the atmosphere, resulting in improved short-term forecasts. In Phase I, the AMU configured a prototype LDIS using the Advanced Regional Prediction System (ARPS) Data Analysis System (ADAS). In Phase II, the AMU simulated a real-time LDIS configuration using two weeks of archived data. In Phase III, the AMU provided assistance to SMG and NWS MLB to install a working real-time LDIS that routinely generates high-resolution products for operational guidance. Based on the examination of real-time analysis output, both SMG and the NWS MLB forecasters have identified several issues that limit the utility of the analyses for evaluating Space Shuttle FR and forecasting problems of east-central Florida. As a result, the LDIS Phase IV task involves modifying the ADAS ingest to include additional real-time observational data sets, fine-tuning the analysis configuration to improve continuity and the blending of observations, and improving real-time graphics capabilities.

A real-time data converter for the RUC model forecasts in hybrid coordinates was tested and installed at the NWS MLB office. The ADAS background fields were transitioned from the pressure-coordinate RUC to the hybrid-coordinate RUC forecasts in order to improve the representation of background variables near the surface. Based on qualitative comparisons of the output, the surface temperature analyses looked more realistic using the hybrid-coordinate RUC data. In addition, scripts were modified to incorporate old RUC grid forecasts at NWS MLB in the event that the most recent RUC forecast data are missing.

The ADAS source code was modified to incorporate temperature and moisture observations from the KSC/CCAFS wind-tower network. Previously, most KSC/CCAFS tower observations of temperature and moisture could not be analyzed by ADAS because of the lack of surface pressure observations. To amend this problem, the observed pressure was estimated by interpolating the RUC background data to the location and height of the KSC/CCAFS wind-tower sensors. The resulting errors in observed temperature and moisture are typically less than 1%. Finally, a problem with the incorporation of pressure observations at surface stations was corrected.

Mr. Case collaborated with the NWS MLB and SMG on two conference papers that were submitted to the AMS joint conference on Numerical Weather Prediction and Weather Analysis and Forecasting. Mr. Case is a co-author on both papers, which will be presented at the upcoming AMS conference in Ft. Lauderdale, FL from 30 July to 2 August. These conference papers represent the final efforts for LDIS Phase III, and describe the aspects of the real-time ADAS as run at SMG and the NWS MLB offices. Mr. Case also submitted an abstract that was accepted by the National Weather Association for the upcoming annual meeting to be held in Spokane, WA from 13–19 October 2001.

SUBTASK 11 EXTENSION / ENHANCEMENT OF THE ERDAS RAMS EVALUATION (MR. CASE AND MR. DIANIC)

The Extension / Enhancement of the ERDAS RAMS Evaluation is being funded by KSC under AMU option hours. During the course of the evaluation under Subtask 8 (Meso-Model Evaluation), the AMU discovered a systematic low-level cold bias in the RAMS forecasts. In addition, several RAMS forecasts were not successfully run in real-time due to various technical issues. As a result, KSC tasked the AMU to re-run historical RAMS forecasts to improve the archived database, and to perform sensitivity tests to identify the possible cause(s) for the model cold bias. Also, depending on the remaining funds in the options hours task, the AMU will explore the possibility of transferring real-time RAMS forecasts to the NWS MLB and SMG offices, and to improve the ENSCO-generated graphical user interface that verifies RAMS forecasts in real time.

Mr. Dianic worked on improvements to the RAMS real-time verification GUI. He fixed a problem in the software that caused the GUI to crash periodically. He also improved various aspects of the interface including the parameter selection menu for the verification of RAMS forecasts at specific instrument sensors. As a result of this improvement, only meteorological parameters that can be measured by the user-selected instrument sensor will be displayed on the GUI. He also modified the time-stepping and display controls to simplify their use. Each of these changes will be tested and implemented for the GUI that currently runs on a workstation in the Range Weather Operations at CCAFS.

Mr. Dianic also incorporated and modified a program that calculates error statistics for RAMS forecasts in order to generate intermediate files for use by the verification GUI. This statistical program will run in conjunction with the verification GUI to provide RMS errors and biases of point forecasts in a graphical format for the current forecast, as well as the previous 30 RAMS forecasts collectively.

2.4 AMU CHIEF'S TECHNICAL ACTIVITIES (DR. MERCERET)

Dr. Merceret managed the final field campaign of the ABFM program, and participated as a scientist at the ground control station. The campaign was completed 30 June. Dr. Merceret, Dr. Manobianco, and Mr. Prasan Chintawongvanich are co-authors on a manuscript in preparation describing the development (by Mr. Chintawongvanich) and evaluation (by the AMU) of a new SODAR technology called "HyperSODAR".

2.5 TASK 001 AMU OPERATIONS

Ms. Lambert visited the SMG at Johnson Space Center (JSC) from 16 - 20 April to observe weather operations in support of the Space Transportation System (STS) 100 launch. While at JSC, Ms. Lambert presented the results from the AMU's Statistical Short-Range Forecast Tools task. She also focused on observing the duties of the Transoceanic Abort Landing sites forecaster. Overall, the visit helped maintain the two-way flow of information between SMG and the AMU by face-to-face discussions of work that is usually described only through written reports.

Mr. Wheeler completed the AMU Information Technology (IT) purchases for this year by submitting two purchase requests (PRs) to the KSC procurement office. The IT items included in the PRs were a Hewlett Packard (HP) workstation and HP software support. He received, installed, and linked the new HP system to the AMU network. After testing, he set up the user accounts, network configuration, and disk cross mounts. The old HP workstation was transferred to the Air Force for their use. Mr. Wheeler also installed, linked to the network and tested the AMU's new LINUX cluster. User accounts and network configuration issues will be addressed in the next quarter. Benchmarking of the cluster will be started in the next few months and will assess the performance of model codes such as the ARPS. The software will be running in parallel on multiple processors across the high-speed network connecting each node of the cluster.

NOTICE

Mention of a copyrighted, trademarked, or proprietary product, service, or document does not constitute endorsement thereof by the author, ENSCO, Inc., the AMU, the National Aeronautics and Space Administration, or the United States Government. Any such mention is solely for the purpose of fully informing the reader of the resources used to conduct the work reported herein.

List of Acronyms

30 SW	30th Space Wing
30 WS	30th Weather Squadron
45 LG	45th Logistics Group
45 OG	45th Operations Group
45 SW	45th Space Wing
45 SW/SE	45th Space Wing/Range Safety
45 WS	45th Weather Squadron
ABFM	Airborne Field Mill
ADAS	ARPS Data Analysis System
AFIT	Air Force Institute of Technology
AFRL	Air Force Research Laboratory
AFSPC	Air Force Space Command
AFWA	Air Force Weather Agency
AMS	American Meteorological Society
AMU	Applied Meteorology Unit
ARPS	Advanced Regional Prediction System
AWIPS	Advanced Weather Interactive Processing System
B	Bias Score
CCAFS	Cape Canaveral Air Force Station
CSI	Critical Success Index
CSR	Computer Sciences Raytheon
ECSB	East Coast Sea Breeze
EOM	End of Mission
ERDAS	Eastern Range Dispersion Assessment System
FAR	False Alarm Rate
FR	Flight Rules
FSL	Forecast Systems Laboratory
FSU	Florida State University
FY	Fiscal Year
GOES	Geostationary Operational Environmental Satellite
GUI	Graphical User Interface
HP	Hewlett Packard
HR	Hit Rate
HSS	Heidke Skill Score
IT	Information Technology
JSC	Johnson Space Center
KSC	Kennedy Space Center
KSS	Kuipers Skill Score
LCC	Launch Commit Criteria
LDIS	Local Data Integration System
LPLWS	Launch Pad Lightning Warning System

List of Acronyms

LWO	Launch Weather Officer
McIDAS	Man-computer Interactive Data Access System
MIDDS	Meteorological Interactive Data Display System
MSE	Mean Square Error
MSFC	Marshall Space Flight Center
NASA	National Aeronautics and Space Administration
NCAR	National Center for Atmospheric Research
NOAA	National Oceanic and Atmospheric Administration
NSSL	National Severe Storms Laboratory
NWP	Numerical Weather Prediction
NWS MLB	National Weather Service in Melbourne, FL
NPTPI	Neumann-Pfeffer Thunderstorm Probability Index
OBS	Observations-Based equations
PCL	Persistence Climatology equations
POD	Probability of Detection
RAMS	Regional Atmospheric Modeling System
RMS	Root Mean Square
RSA	Range Standardization and Automation
RTLS	Return to Launch Site
RUC	Rapid Update Cycle
SLF	Shuttle Landing Facility
SLTI	Stratified Logistic Thunderstorm Index
SMC	Space and Missile Center
SMG	Spaceflight Meteorology Group
SRH	NWS Southern Region Headquarters
STS	Space Transportation System
TS	Threat Score
USAF	United States Air Force
UTC	Universal Coordinated Time
WSR-74C	Weather Surveillance Radar, model 74C
WSR-88D	Weather Surveillance Radar 1988 Doppler
WWW	World Wide Web

Appendix A

AMU Project Schedule 31 July 2001				
AMU Projects	Milestones	Scheduled Begin Date	Scheduled End Date	Notes/Status
Statistical Forecast Guidance (Ceilings)	Determine Predictand(s)	Aug 98	Sep 98	Completed
	Data Collection, Formulation and Method Selection	Sep 98	Apr 99	Completed
	Equation Development, Tests with Independent Data, and Tests with Individual Cases	Apr 00	Dec 00	Completed
	Prepare Products, Final Report for Distribution	Jan 00	Jun 01	Behind Schedule – Task lead on extended leave due to family emergency
Statistical Forecast Guidance (Winds)	Determine Predictand(s)	Jun 01	Jun 01	Behind Schedule – Waiting to complete ceiling stats task
	Data Reduction, Formulation and Method Selection	Jun 01	Jul 01	Behind Schedule – Waiting to complete ceiling stats task
	Equation Development, Tests with Independent Data, and Tests with Individual Cases	Jul 01	Sep 01	On Schedule
	Prepare Products, Final Report for Distribution	Sep 01	Dec 01	On Schedule
Meso-Model Evaluation	Develop ERDAS/RAMS Evaluation Protocol	Feb 99	Mar 99	Completed
	Perform ERDAS/RAMS Evaluation	Apr 99	Sep 99	Completed
	Extend ERDAS/RAMS Evaluation	Oct 99	Nov 00	Completed
	Interim ERDAS/RAMS Report	Dec 99	Aug 00	Completed
	Final ERDAS/RAMS Report	Oct 00	Jun 01	Completed
LDIS Extension: Phase IV	Modify ADAS ingest to include additional data sets	May 01	Oct 01	On Schedule
	Fine-tune ADAS configuration	May 01	Oct 01	On Schedule
	Improve visualization tools	May 01	Oct 01	On Schedule
	Memorandum summarizing modified ADAS configuration and task issues	Nov 01	Nov 01	On Schedule

AMU Project Schedule

31 July 2001

AMU Projects	Milestones	Scheduled Begin Date	Scheduled End Date	Notes/Status
ERDAS RAMS Extension Task	Memorandum summarizing data transfer feasibility to SMG & NWS MLB	Jul 00	May 01	Completed
	Enhancement of verification Graphical User Interface	Apr 00	Jul 01	Behind Schedule-- Data recovery took longer than expected
	Develop data transfer	Sep 00	Mar 01	Completed
	Input of methodology and results into ERDAS RAMS final report	Nov 00	Mar 01	Completed
Improved Anvil Forecasting Phase II	Collection and processing of data	May 01	Aug 02	On Schedule
	Algorithm formulation and testing	Aug 01	May 02	On Schedule
	Final Report	May 02	Aug 02	On Schedule
Neumann-Pfeffer TSTM Probability Index	Convert Software	Oct 01	Jan 01	Completed
	Write data decoders, transition to RWO PC, and prepare documentation	Jan 01	Jun 01	Completed